Theoretical Evaluation of the Distributed Power Dissipation in Biological Cells Exposed to Electric Fields

Tadej Kotnik[1,2] and Damijan Miklavčič[1]*

[1]*University of Ljubljana, Faculty of Electrical Engineering, Ljubljana, Slovenia*
[2]*PPMB/UMR 8532 CNRS, Institut Gustave-Roussy, Villejuif, France*

The paper deals with the power dissipation caused by exposure of biological cells to electric fields of various frequencies. With DC and sub-MHz AC frequencies, power dissipation in the cell membrane is of the same order of magnitude as in the external medium. At MHz and GHz frequencies, dielectric relaxation leads to dielectric power dissipation gradually increasing with frequency, and total power dissipation within the membrane rises significantly. Since such local increase can lead to considerable biochemical and biophysical changes within the membrane, especially at higher frequencies, the bulk treatment does not provide a complete picture of effects of an exposure. In this paper, we theoretically analyze the distribution of power dissipation as a function of field frequency. We first discuss conductive power dissipation generated by DC exposures. Then, we focus on AC fields; starting with the established first-order model, which includes only conductive power dissipation and is valid at sub-MHz frequencies, we enhance it in two steps. We first introduce the capacitive properties of the cytoplasm and the external medium to obtain a second-order model, which still includes only conductive power dissipation. Then we enhance this model further by accounting for dielectric relaxation effects, thereby introducing dielectric power dissipation. The calculations show that due to the latter component, in the MHz range the power dissipation within the membrane significantly exceeds the value in the external medium, while in the lower GHz range this effect is even more pronounced. This implies that even in exposures that do not cause a significant temperature rise on the macroscopic, whole-system level, the locally increased power dissipation in cell membranes could lead to various effects at the microscopic, single-cell level. Bioelectromagnetics 21:385-394, 2000.   © 2000 Wiley-Liss, Inc.

INTRODUCTION

Power Dissipation and Temperature Increase Caused by Exposure to Electric Fields

Exposure of biological cells to electric fields can lead to a variety of profound biochemical and biophysical effects. In general, evaluation of these effects is based on the power dissipation caused by the exposure. For an electric field E, the power dissipation per unit volume is given by

$$P = \sigma \overline{E}^2, \tag{1}$$

where $\overline{E}$ is the effective value of the field ($\overline{E} = E$ for DC fields, and $\overline{E} = E/\sqrt{2}$ for AC fields). A related quantity often used is the power dissipation per unit mass, also known as the specific absorption rate (SAR), which is P (as in Equation 1) divided by the density of the material.

At sub-MHz frequencies, an exposure to electric field results in *conductive power dissipation*, caused by the translational friction of current carriers (ions in electrolyte solutions). With fields in the MHz and GHz range, an additional component of power dissipation caused by rotation or flexion of molecular dipoles

(dielectric relaxation) becomes relevant. With increase in frequency, this component, known as *dielectric power dissipation*, ultimately prevails. Separate treatment of the two components of power dissipation is elegantly avoided by the introduction of effective conductivity $\sigma(\omega)$ and effective dielectric permittivity $\varepsilon(\omega)$ of the material. These two terms can be written as

$$\sigma(\omega) = \sigma(0) + \omega \sum_{k=1}^{n} \frac{\Delta \varepsilon_k \omega \tau_k}{1 + \omega^2 \tau_k^2}, \tag{2a}$$

$$\varepsilon(\omega) = \varepsilon(0) - \sum_{k=1}^{n} \frac{\Delta \varepsilon_k \omega^2 \tau_k^2}{1 + \omega^2 \tau_k^2}, \tag{2b}$$

where $\omega = 2\pi\nu$, with ν denoting the frequency of the field, n is the number of steps of dielectric relaxation of the material, $\Delta \varepsilon_k$ is the magnitude of the k-th relaxation step, τ_k is the time constant of the k-th step, while $\sigma(0)$ and $\varepsilon(0)$ are respectively the conductivity and dielectric permittivity of the material (values measured at $\omega \ll 1/\tau_1$).

Thus, Equation 1 can be rewritten to give the combined conductive and dielectric power dissipation at a given frequency

$$P(\omega) = \sigma(\omega)\overline{E}^{\,2}, \tag{3}$$

where $\sigma(\omega)$ is given by Equation 2a, and $\overline{E}$ is the effective value of the field. With no heat flow, an exposure of duration Δt would result in a temperature increase

$$\Delta T(\omega) = P(\omega) \cdot \frac{\Delta t}{\rho \cdot c_P}, \tag{4}$$

where ρ is the density, and c_P the heat capacity of the material. This is, however, not the case with cell suspensions or tissues, where heat flow is always present and results in heat redistribution. Therefore, while Equation 3 correctly describes the power dissipation, the resulting temperature increase in each particular region is much less straightforward to determine and can be approximated as proportional to the power dissipation only for very short exposures, where heat transfer is negligible [Foster et al., 1998]. Thus, in this paper we focus exclusively on the power dissipation predicted by various physical models.

Another comment should be made before we proceed. Any time-varying electric field is coupled to a magnetic field, and besides non-zero conductivity and dielectric permittivity, any real material also has a non-zero magnetic permeability. This leads to eddy currents and to *magnetic power dissipation*. This component is significant in materials with high magnetic permeability, especially ferromagnetics. Biological materials, on the other hand, are characterized by very low magnetic permeabilities, and magnetic power dissipation is negligible in comparison to the other two components. Henceforth, we deal only with conductive and dielectric power dissipation.

Advantages of the Distributed Treatment

Usually, power dissipation is assessed through the bulk properties of the tissue or cell suspension: the bulk conductivity is used in calculation of the conductive component, and the bulk dielectric relaxation in calculation of the dielectric component. This ignores any nonuniformities in the distribution of electric field strength, electric current density, and hence of power dissipation. Such nonuniformities do, however, undoubtedly exist at the macroscopic (tissue) level, e.g. due to the blood vessels or adipose regions within the tissue, as well as at the microscopic (single-cell) level, since electrical properties of the cell membrane differ significantly from both cell interior and exterior. The bulk treatment thus provides a valid estimate of the total heat released in the exposed tissue or cell suspension as a whole, but does not address the localized differences in power dissipation in distinct subregions within the exposed object.

Nonuniformities in power dissipation, however, can be substantial. An important example, as will be corroborated later, is the local increase of power dissipation within the plasma membrane in the higher MHz frequency range. Because of the extremely small relative volume occupied by the membrane, a significantly higher power dissipation per unit volume within the membrane does not show on the macroscopic level. Nevertheless, it could cause damage to the constituents of the membrane.

In this paper, we theoretically evaluate the distribution of the power dissipation on the single-cell level. The analytical approach we present applies strictly only to relatively low cell densities, such as those found in cell suspensions. Qualitatively, however, the conclusions obtained by this model can be extrapolated to denser cell distributions in tissues.

MODELS OF POWER DISSIPATION

The Static Model

We first focus on the model that treats the cells exposed to a DC electric field. For a spherical cell with

a uniform membrane, the membrane voltage induced by an external DC field of amplitude E_e is given by

$$U_m(\theta) = f_S E_e R \cos\theta, \tag{5}$$

with R denoting the cell radius, θ the polar angle measured with respect to the direction of the field, and f_S given by [Kotnik et al., 1997]

$$f_S = \frac{3\sigma_e[3dR^2\sigma_i + (3d^2R - d^3)(\sigma_m - \sigma_i)]}{2R^3(\sigma_m + 2\sigma_e)(\sigma_m + \frac{1}{2}\sigma_i) - 2(R-d)^3(\sigma_e - \sigma_m)(\sigma_i - \sigma_m)}, \tag{6}$$

where σ_i, σ_m and σ_e are DC conductivities of the cytoplasm, membrane, and cell exterior, respectively, and d is the membrane thickness (see also Fig. 1).

Under physiological conditions, where $\sigma_i, \sigma_e \gg \sigma_m$ and $R \gg d$ (see Table 1), the term f_S can be approximated by a constant, $f_S \doteq 1.5$, and the error thus committed never exceeds several parts in a thousand. Nevertheless, many experiments *in vitro* make use of low-conductivity media, in which this simplification does not apply [Kotnik et al., 1997]. To keep these experiments in scope, we deal with the general case, while in physiological conditions f_S can always be given the value of 1.5.

From this point on, we focus on the situation at $\theta = 0$, i.e. at the tip of the membrane facing the positive electrode (point A in Fig. 1), where the induced transmembrane voltage has a maximum. We denote $U_m \equiv U_m(\theta = 0)$, and hence

$$U_m = f_S E_e R. \tag{7}$$

For a homogeneous membrane, the membrane electric field is then

$$E_m = \frac{U_m}{d} = \frac{f_S E_e R}{d}, \tag{8}$$

and, by Equation 3, the power dissipation in the membrane is given by

$$P_m = \sigma_m \overline{E}_m^2 = \frac{\sigma_m f_S^2 E_e^2 R^2}{d^2}, \tag{9}$$

while the power dissipation in the surrounding medium equals

$$P_e = \sigma_e \overline{E}_e^2 = \sigma_e E_e^2. \tag{10}$$
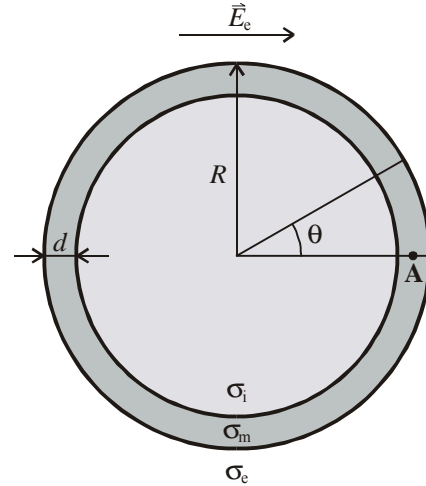

Fig. 1: The static model of the cell.

Using typical parameter values (Table 1) and an arbitrarily chosen field amplitude $E_e = 100$ V/cm, from Equations 9 and 10 we get $P_m = 2.7 \times 10^8$ W/m^3 and $P_e = 1.2 \times 10^8$ W/m^3. Since the ratio P_m/P_e is independent of E_e, this simple example shows that in DC fields, the power dissipation in the membrane is typically somewhat higher than the power dissipation in the surrounding medium. As the two quantities are of the same order of magnitude, the bulk treatment can be utilized in determining the thermal effects of exposure at least to get a rough estimate. Due to the shielding effect of the membrane in DC fields, power dissipation in the cytoplasm (P_i) is many orders of magnitude smaller than both P_e and P_m.

There are at least two factors that distinguish a DC exposure from an AC exposure. First, exposure to a DC field does not result in a direct current through the exposed object, but only produces a brief current of polarization. A direct current only arises if the exposed object is in a conductive contact with the DC voltage source. Unlike that, exposure to an AC field creates an alternating current in the exposed object. Even though an exposure to a continuous direct current could be devised, the real-life cases of DC exposure are mostly limited to discharges that occur when the object comes into a contact with a charged material, and power dissipation is caused by the transient current of discharge.

Second, a DC exposure is always accompanied by electrolytic effects. Both the material released from electrodes and electrochemical changes in the medium modify the conductivities within the exposed suspension or tissue. Generally, the longer the exposure, the larger the change of conductivity. This denies the validity of the DC model in evaluation of the power

TABLE 1. Values Used in the Calculations

Parameter	Symbol	Value	Reference
Cell radius	R	10 μm	
Membrane thickness	d	5 nm	Alberts et al., 1994
Cytoplasm conductivity	σ_i	0.3 S/m	Harris and Kell, 1983; Hölzel and Lamprecht, 1992
Membrane conductivity	σ_m	3×10^{-7} S/m	
			Gascoyne et al., 1993
Extracellular medium conductivity	σ_e	1.2 S/m	Sunderman, 1945[a]
Cytoplasm permittivity	ε_i	6.4×10^{-10} As/Vm	see ε_e
Membrane permittivity	ε_m	4.4×10^{-11} As/Vm	from Gascoyne et al., 1993 ($\varepsilon_m/\varepsilon_0 = 5.0$)
Extracellular medium permittivity	ε_e	6.4×10^{-10} As/Vm	from Büchner et al., 1999[b] ($\varepsilon_e/\varepsilon_0 = 72.5$)

[a]Conductivity of blood serum at 35°C   [b]Permittivity of 0.154 M NaCl at 35°C

dissipation, except for exposures lasting up to several milliseconds.

The First-Order Model

Unlike the static model, the first-order model [Pauly and Schwan, 1959] treats the membrane as a lossy dielectric (a material with both non-zero conductivity σ_m and dielectric permittivity ε_m), while the cytoplasm and the external medium are still assumed to have a purely conductive character (Fig. 2a).

The amplitude of the induced membrane voltage at $\theta = 0$ is expressed analogously to Equation 5

$$U_m(\omega) = F_{S1} E_e R, \tag{11}$$

where F_{S1} is obtained from f_S as given by (6) if membrane conductivity is replaced by membrane admittivity $(\sigma_m + j\omega\varepsilon_m)$; E_e is still the amplitude of the external field. This simple approach limits the analysis to the steady state of AC exposure (which is in the scope of this paper), while the treatment of the transients requires a different technique and is explained elsewhere [Kotnik et al., 1998].

While Equation 11 gives a precise result and is effortlessly handled by a computer, there is a feasible approximation [Pauly and Schwan, 1959]

$$U_m(\omega) \doteq f_S E_e R \frac{1}{1 + j\omega\tau_m}, \tag{12}$$

where f_S is given by Equation 6, with $f_S \doteq 1.5$ in physiological conditions, while τ_m is the time constant of the membrane, approximated by

$$\tau_m \doteq \frac{\varepsilon_m}{\dfrac{d}{R}\dfrac{2\sigma_i\sigma_e}{\sigma_i + 2\sigma_e} + \sigma_m}. \tag{13}$$

We proceed as in the static case, but with effective field values obeying $\overline{E} = E/\sqrt{2}$, and obtain

$$P_m(\omega) = \sigma_m \overline{E}_m^2 \doteq \sigma_m \frac{f_S^2 E_e^2 R^2}{2d^2(1 + 2j\omega\tau_m - \omega^2\tau_m^2)}, \tag{14}$$

$$P_e = \sigma_e \overline{E}_e^2 = \frac{\sigma_e E_e^2}{2}. \tag{15}$$

For the numerical evaluation of the first-order model, we choose the same parameter values as in the static model, except for E_e, which we now set at $\sqrt{2} \times 100$ V/cm in order to obtain the same effective value of 100 V/cm as in the DC case. Figure 2b shows that up to the higher kHz range, the amplitude of the induced membrane voltage remains constant (the low-frequency plateau), while above the breakpoint frequency $\nu_m = 1/(2\pi\tau_m)$, it decreases linearly with increase of frequency. This also affects the power dissipation within the membrane, which according to the first-order model becomes negligible at frequencies above 1 MHz (Fig. 2c). In contrast, power dissipation in the external medium is frequency independent. As in the static model, power dissipation in the cytoplasm at low frequencies is negligible, but in the upper kHz range and above, as the shielding effect of the membrane is progressively attenuated, P_i gradually increases until it finally reaches 25% of P_e (the ratio of conductivities σ_i/σ_e). The first-order model ignores capacitive properties of both cytoplasm and external medium; in addition, it only accounts for conductive power dissipation. As will be shown shortly, this makes the first-order model of power dissipation applicable only to sub-MHz frequencies.

The Second-Order Model

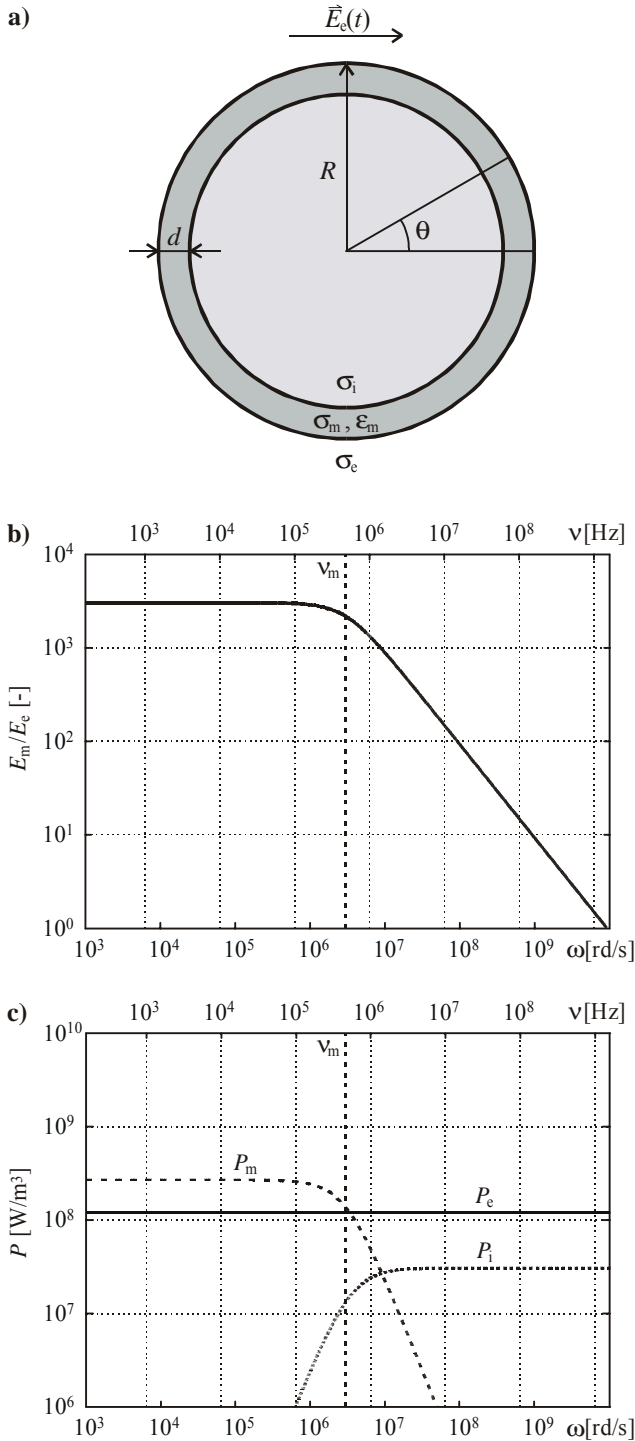Assignment of nonzero conductivities and dielectric permittivities to all regions (Fig. 3a) leads to a

a)

b)

c)

Fig. 2. The first-order model: (**a**) model of the cell; (**b**) E_m/E_e as a function of frequency; (**c**) P_i, P_m and P_e at $E_e = \sqrt{2} \times 100$ V/cm as functions of frequency. The bold dotted vertical is at the breakpoint frequency $\nu_m = 1/(2\pi\tau_m)$. Parameter values used in the calculations are given in Table 1.

broader, second-order model of induced membrane voltage [Kotnik et al., 1998]. For a sinusoidal electric field, this model describes U_m as

$$U_m(\omega) = F_{S2} E_e R, \qquad (16)$$

with F_{S2} obtained from f_S of Equation 6 by replacing all three conductivities with the corresponding admittivities: $\sigma_i \rightarrow \sigma_i + j\omega\varepsilon_i$; $\sigma_m \rightarrow \sigma_m + j\omega\varepsilon_m$; $\sigma_e \rightarrow \sigma_e + j\omega\varepsilon_e$. As with the first-order model, this approach addresses the steady state of AC exposure, while the analysis of transients is described in [Kotnik et al., 1998].

Again, (16) presents no serious challenge for a computer, but can be approximated as

$$U_m(\omega) \doteq f_S E_e R \frac{1 + j\omega\tau_{m2}}{1 + j\omega\tau_{m1}}, \qquad (17)$$

where f_S is given by Equation 6, with $f_S \doteq 1.5$ in physiological conditions, while the first time constant of the membrane τ_{m1} is approximated by the same expression as τ_m of Equation 13, and the second time constant of the membrane τ_{m2} is approximated by

$$\tau_{m2} \doteq \frac{\varepsilon_i + 2\varepsilon_e}{\sigma_i + 2\sigma_e}. \qquad (18)$$

As shown in Figure 3b, the most important difference between the first- and second-order model is the prediction of the latter that the decrease of induced voltage with frequency comes to a halt after a second breakpoint frequency $\nu_{m2} = 1/(2\pi\tau_{m2})$, reaching a high-frequency plateau. According to the second-order model, this leads to a similar halt of the decrease of the membrane power dissipation, but at $P_m \approx 6300$ W/m^3 (out of the range of Fig. 3c), which is over 40000 times smaller than the low-frequency P_m and almost 20000 times smaller than P_e. Predictions regarding P_i are very similar to those of the first-order model.

Unlike the first-order model, the second-order model treats all the regions of the system as having both conductive and capacitive properties, which extends the model's frequency range in prediction of the induced membrane voltage up to hundreds of MHz. However, its predictions regarding power dissipation are very similar to the first-order model, since it still involves only the conductive component of power dissipation. To include the dielectric component, effects of dielectric relaxation must be introduced. We do this in the next subsection.
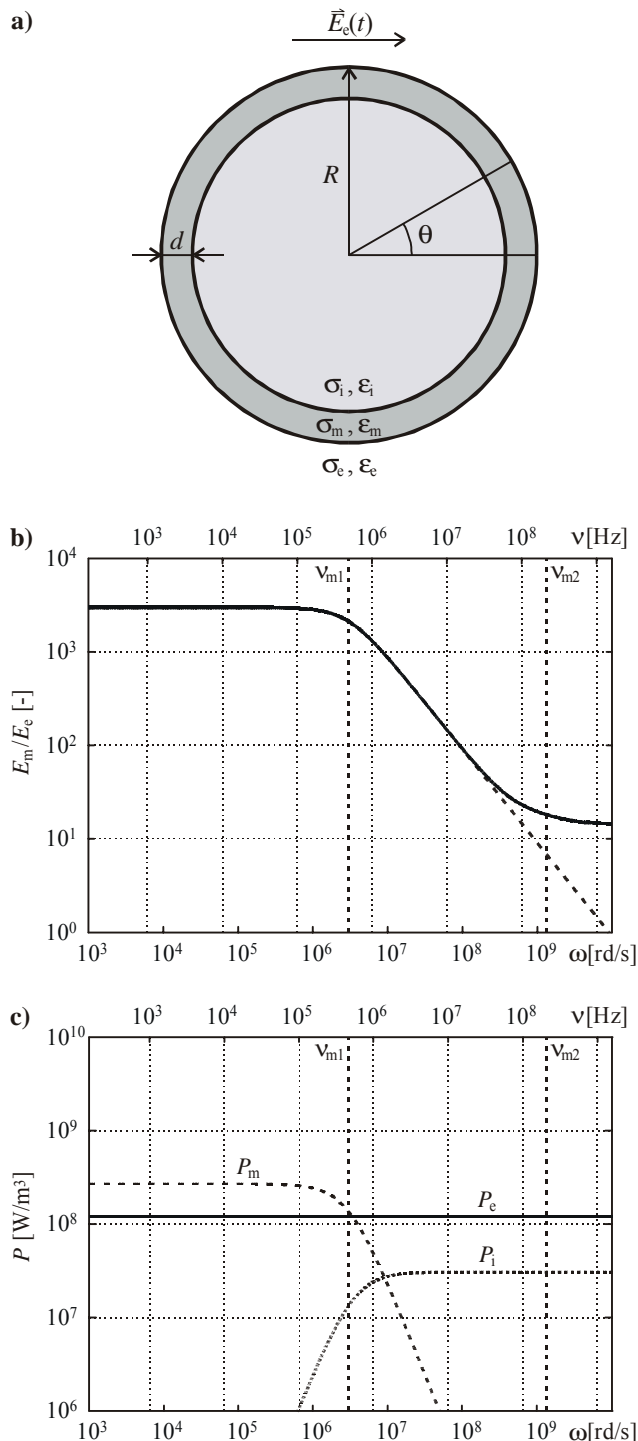
a)

b)

c)

Fig. 3. The second-order model: (**a**) model of the cell; (**b**) E_m/E_e as a function of frequency (solid) and the corresponding prediction of the first-order model (dashed); (**c**) P_i, P_m and P_e at $E_e = \sqrt{2} \times 100$ V/cm as functions of frequency. The two bold dotted verticals indicate the first and the second breakpoint frequency, $\nu_{m1} = 1/(2\pi\tau_{m1})$ and $\nu_{m2} = 1/(2\pi\tau_{m2})$. Parameter values used in the calculations are given in Table 1.

The Enhanced Second-Order Model with Dielectric Relaxation

With validity of the second-order model extended to higher frequencies than the first-order model, an upper limit for its reliable use is imposed by the processes of dielectric relaxation. Due to these processes, the effective conductivity of the materials experiences sigmoidal ascents with increasing frequency as described by Equation 2a, and is coupled to sigmoidal descents in the respective effective permittivity according to Equation 2b. Increase of effective conductivity due to dielectric relaxation is the basis of dielectric power dissipation, which is today used in many applications; microwave ovens are probably the best known among them.

While dielectric relaxation of water molecules and dissolved ions, which are the predominant constituents of cytoplasm and cell exterior, only starts in the GHz region, effects of dielectric relaxation of the membrane already emerge in the range of tens to hundreds of MHz [Nimtz et al., 1985; Klösgen et al., 1996]. The main reason for this is the limited rotational mobility of headgroups of membrane lipids.

Precise data on relaxation of aqueous salt solutions have become relatively abundant in the last two decades. Regrettably, this is not the case for lipid bilayers, where direct measurements remain very scarce. Results have been published on relaxation of colloidal suspensions of lipid vesicles [Pottel et al., 1984], homogenized samples with various water-lipid molecular ratios [Nimtz et al., 1985] and more recently on multilamellar bilayer samples [Klösgen et al., 1996]. An alternative, indirect approach to the determination of relaxation data for lipid bilayers is provided by the P-NMR and ^{2}H-NMR measurements of headgroup mobility [Dufourc et al., 1992; Ulrich and Watts, 1994]. We base a provisional estimate of the data of lipid bilayer relaxation on [Klösgen et al., 1996], while dielectric spectra of the cytoplasm and the extracellular medium are those of physiological saline (0.154 M NaCl) at 35°C taken from [Büchner et al., 1999] (Table 2). The choice of physiological saline as an approximation of the extracellular medium and the cytoplasm is reasonable, as isotonic aqueous salt solution is the major constituent of both cytoplasm and extracellular medium. We must note that while the latter data are reliable, data regarding lipid bilayer relaxation are much more tentative. In the experiment by Klösgen et al. [1996], the bilayer lamellae were not parallel and did not spread throughout the sample. Electric currents flowing around them could lead to structural relaxation superimposed upon material
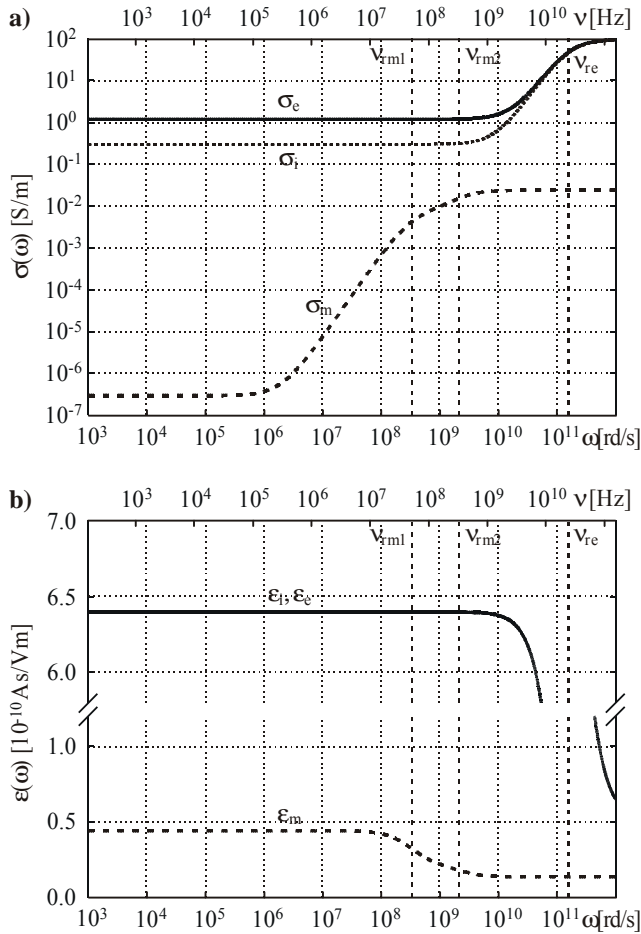
Fig. 4. Cytoplasmic, membrane and extracellular effective conductivities (**a**) and effective permittivities (**b**) as functions of field frequency. Parameter values used in the calculations are given in Tables 1 and 2.

relaxation, making extrapolation of these data to a single bilayer questionable.

Figure 4 plots the effective conductivities (Fig. 4a) and effective permittivities (Fig. 4b) of the model as functions of frequency. It shows that the effective

value of σ_m becomes frequency-dependent in the lower MHz range, while for the effective values of σ_i and σ_e field frequency only starts to play a role in the GHz region. Altogether, this implies that in the MHz range and above, dielectric relaxation effects (and thereby dielectric power dissipation) must be taken into account for a valid treatment of power dissipation.

The second-order model is easily enhanced to account for dielectric relaxation by replacing absolute conductivities and dielectric permittivities by their effective, frequency-dependent counterparts (Fig 5a). Then,

$$U_m(\omega) = F_{S(2+DR)} E_e R, \qquad (19)$$

where $F_{S(2+DR)}$ is analogous to F_{S2}, but contains effective conductivities and permittivities instead of absolute ones. With f_S of Equation 6 as a starting point, $F_{S(2+DR)}$ is thus obtained by substituting: $\sigma_i \rightarrow \sigma_i(\omega) + j\omega\varepsilon_i(\omega)$; $\sigma_m \rightarrow \sigma_m(\omega) + j\omega\varepsilon_m(\omega)$; $\sigma_e \rightarrow \sigma_e(\omega) + j\omega\varepsilon_e(\omega)$, where the effective conductivities and permittivities are given by Equations 2a and 2b, respectively, with parameter values as in Table 2.

While $\sigma_m(\omega)$ and $\sigma_e(\omega)$ suggest that dielectric relaxation must be included in a viable model of power dissipation, this receives further support from the calculated frequency dependence of E_m/E_e (Fig. 5b) as well as of P_i, P_m and P_e (Fig. 5c). Comparison of these plots to the corresponding curves in Figures 2 and 3 shows that predictions of power dissipation change dramatically with the introduction of dielectric relaxation. This is due to the fact that while the first- and second-order models account only for conductive component of power dissipation, at higher frequencies the dielectric component is much more important. Increase of the effective σ_m with frequency (see Fig. 4a) counterbalances the decrease of U_m (and thereby E_m) and even leads to increase of P_m; at 1 GHz, P_m exceeds P_e by approximately a factor of 50 (Fig. 5c).

TABLE 2. Parameters of Dielectric Relaxation of Cytoplasm, Membrane, and Extracellular Medium

Parameter	Symbol	Value	Reference
Cytoplasm and extracellular medium			
First relaxation time	τ_{re}	6.2×10^{-12} s	Büchner et al., 1999[a]
First relaxation step	$\Delta\varepsilon_e$	5.9×10^{-10} As/Vm	Büchner et al., 1999[a]
Membrane			
First relaxation time	τ_{rm1}	3.0×10^{-9} s	Klösgen et al., 1996
First relaxation step	$\Delta\varepsilon_{m1}$	2.3×10^{-11} As/Vm	from Klösgen et al., 1996[b]
Second relaxation time	τ_{rm2}	4.6×10^{-10} s	Klösgen et al., 1996
Second relaxation step	$\Delta\varepsilon_{m2}$	7.4×10^{-12} As/Vm	from Klösgen et al., 1996[b]

[a] Permittivity of 0.154 M NaCl at 35°C

[b] Scaled by $\varepsilon_m/\varepsilon = 0.125$, where $\varepsilon_m = 4.4 \times 10^{-11}$ As/Vm is the static permittivity of lipid bilayer (see Table 1), and $\varepsilon = 3.5 \times 10^{-10}$ As/Vm is the static permittivity of the multilamellar sample used by Klösgen et al. [Klösgen et al., 1996]
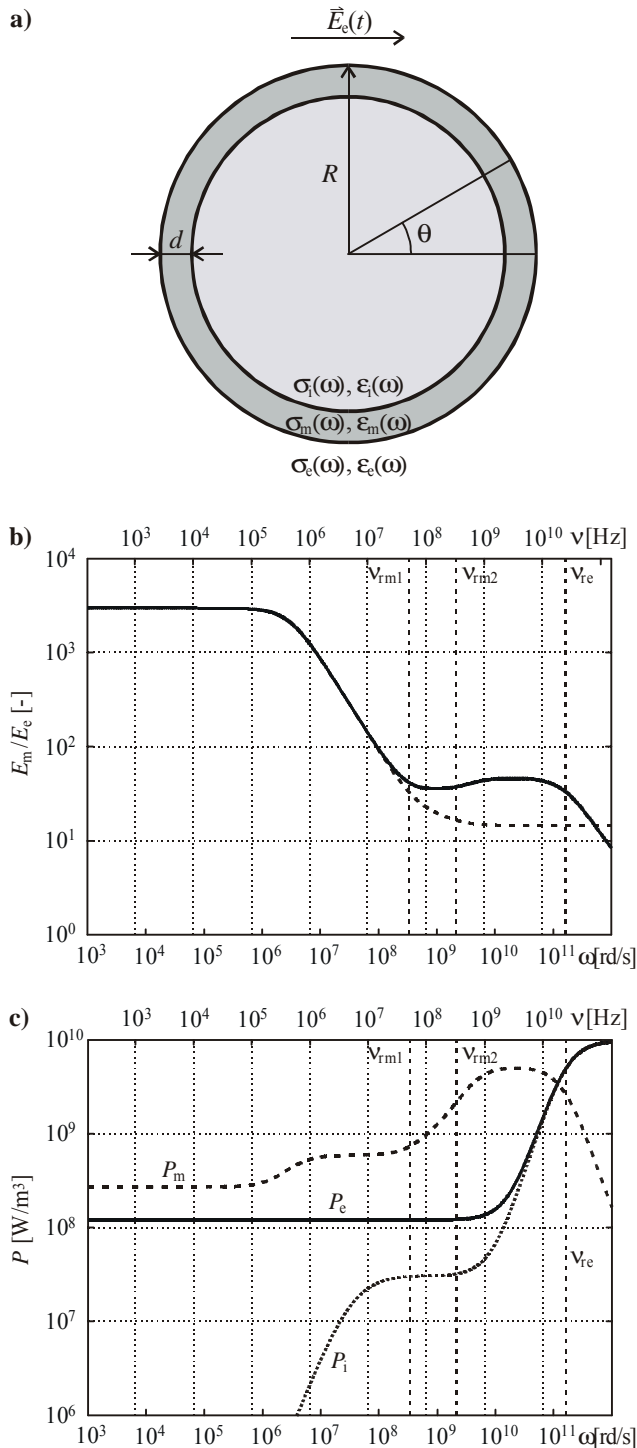
a)

b)

c)

Fig. 5. The enhanced second-order model with dielectric relaxation: (a) model of the cell; (b) E_m/E_e as a function of frequency (solid) and the corresponding prediction of the second-order model without dielectric relaxation (dashed); (c) P_i, P_m and P_e at $E_e = \sqrt{2}$ x 100 V/cm as functions of frequency. The three bold dotted verticals correspond to the relaxation frequencies, from left to right: $\nu_{rm1} = 1/(2\pi\tau_{rm1})$, $\nu_{rm2} = 1/(2\pi\tau_{rm2})$, and $\nu_{re} = 1/(2\pi\tau_{re})$. Parameter values used in the calculations are given in Tables 1 and 2.

Above 1 GHz, dielectric relaxation of water and dissolved ions causes a gradual increase of P_i and P_e, while P_m reaches a plateau and then starts decreasing to be ultimately exceeded by P_i and P_e at frequencies above 20 GHz.

DISCUSSION

We presented four different models of power dissipation. It is now time to discuss the range of valid application for each of these models. While a DC exposure always results in a purely conductive power dissipation, electrolytic effects change the electrical and chemical properties of exposed tissues or cell suspensions. This makes the application of the DC model questionable, and in addition, when a damaging effect of a DC exposure is evaluated, electrochemical changes might be more detrimental to exposed cells than power dissipation itself.

On the other hand, power dissipation generated by an AC exposure is of a composite nature; with increase in frequency, the conductive component remains stable and then starts to decline, while the dielectric component gradually gains importance, until in the MHz to GHz range it eventually exceeds by far the conductive component. The first-order model appropriately describes the induced membrane voltage and membrane field below the high-frequency plateau, i.e., up to about 30 MHz, while its prediction of power dissipation is limited to the range where the conductive component is predominant, up to ~100 kHz. Extended by the permittivities of the aqueous regions, the second-order model validly describes the induced membrane voltage and field up to about 100 MHz, but since it still does not involve dielectric power dissipation, its ability to predict the power dissipation is practically the same as that of the first-order model. This deficiency is surmounted by introducing the dielectric relaxation through the effective, frequency-dependent values of the conductivities and permittivities. Therefore, only enhancement of the second-order model by inclusion of the effects of dielectric relaxation enables correct assessment of power dissipation at frequencies above 100 kHz.

Since the first- and second-order models seem equally inadequate to describe dielectric power dissipation, it might be necessary to explain the choice of the second-order model as a starting point for a model with dielectric relaxation. As Equation 3 shows, with a given material, it is the electric field strength that ultimately determines the power dissipation within the material. Because of this, it is the high-frequency plateau of the induced membrane voltage (and thereby

the induced membrane field) that provides the basis for the increase of membrane power dissipation at high frequencies. In the first-order model, the high-frequency plateau is absent, and the behavior of membrane power dissipation as shown in Fig. 5c is also not anticipated.

The analysis presented in this paper sets two guidelines to the evaluation of effects of exposure to electric fields:

1. For any exposure to electric field, the distributed treatment by means of any of the presented models which is valid for a given exposure gives a more thorough picture than the bulk treatment. Localized differences in the power dissipation should be accounted for, since they might lead to varying degrees of damage in different subregions of the exposed tissues or cell suspensions, especially at the single-cell level. Our calculations show that even at low frequencies, the power dissipation generated in the membrane is higher than that in the external medium.

2. For exposures to fields with frequencies above ~100 kHz, the dielectric component of power dissipation prevails. Therefore, the enhanced second-order model with dielectric relaxation is the only model able to describe the power dissipation at high frequencies. Local increase of power dissipation within the membrane, which is already present at low frequencies, becomes much more pronounced in the MHz and lower GHz regions. At frequencies above 20 GHz, power dissipation within the membrane drops again, while power dissipation within the aqueous media becomes predominant.

It should be stressed that the enhanced second-order model with dielectric relaxation, as the most advanced of the four presented models, is applicable to any exposure that the simpler models can handle, including the DC exposures. Nevertheless, even this model has its limitations. As already noted, parameter values used in numerical calculations that lead to Figures 5b and 5c are partly based on speculative information (extrapolation of relaxation data on multilamellar lipid bilayer stacks to monolamellar lipid bilayers). When reliable data become available, the enhanced second-order model with dielectric relaxation should be valid at least up to tens of GHz. Precise predictions in the range above 100 GHz will probably have to await a new generation of dielectric relaxation measurements. At even higher frequencies, the field wavelength becomes of the order of cell dimensions, and the field starts to exhibit its wave nature. This situation cannot be treated by the enhanced second-order model given by Equation 19 anymore, but requires an evaluation through a completely electrodynamic approach (all presented models disregard the finite speed of electric field propagation and should be, technically speaking, referred to as quasi-static [Johnk, 1988]).

Finally, one must be aware of the fact that the presented evaluation is purely theoretical, and as such necessarily calls for further investigations:

- Experimental tests of the presented theory. While many recent experimental studies have dealt with the macroscopic effects of high-frequency exposures, both whole-body [Adair et al., 1998; Adair et al., 1999] and single-organ [Vollrath et al., 1997; de Seze et al., 1998; Freude et al., 1998; Walters et al., 1998], calculations presented in this paper call for evaluation of effects at a microscopic, single-cell level. If exposures to high-frequency fields actually cause much higher power dissipation in cell membranes than in the cell interior and cell exterior, this could lead to structural changes in membrane proteins and the lipid matrix. This could be verified by various techniques: biochemical analysis of the membrane proteins, measurements of membrane fluidity, conductivity, permeability to different molecules, X-ray and neutron diffraction, etc.

- Precise measurements of dielectric relaxation of lipid bilayers. If the general validity of the presented theory is confirmed, data of higher reliability on the dielectric relaxation of lipid bilayers will offer a basis for an accurate reevaluation of the calculations presented in this paper. In addition to measurements on artificial bilayers with various lipid content, more realistic membrane models involving proteins should also be studied.

REFERENCES

Adair ER, Kelleher SA, Mack GW, Morocco TS. 1998. Thermo-physiological responses of human volunteers during controlled whole-body radio frequency exposure at 450 MHz. Bioelectromagnetics 19:232-245.

Adair ER, Cobb BL, Mylacraine KS, Kelleher SA. 1999. Human exposure at two radio frequencies (450 and 2450 MHz): similarities and differences in physiological response. Bioelectromagnetics 20(suppl. 4):12-20.

Alberts B, Bray D, Lewis J, Raff M, Roberts K, Watson JD. 1994. Molecular biology of the cell, 3rd ed. New York: Garland Publishing, p. 477.

Büchner R, Hefter GT, May PM. 1999. Dielectric relaxation of aqueous NaCl solutions. J Phys Chem A 103:1-9.

de Seze R, Fabbro-Peray P, Miro L. 1998. GSM radiocellular telephones do not disturb the secretion of antepituitary hormones in humans. Bioelectromagnetics 19:271-278.

Dufourc EJ, Mayer C, Stohrer J, Althoff G, Kothe G. 1992. Dynamics of phosphate head groups in biomembranes. Biophys J 61:42-57.

Foster KR, Lozano-Nieto A, Riu PJ, Ely TS. 1998. Heating of tissues by microwaves: a model analysis. Bioelectromagnetics 19:420-428.

Freude G, Ullsperger P, Eggert S, Ruppe I. 1998. Effects of microwaves emitted by cellular phones on human slow brain potentials. Bioelectromagnetics 19:384-387.

Gascoyne PRC, Pethig R, Burt JPH, Becker FF. 1993. Membrane changes accompanying the induced differentiation of Friend murine erythroleukemia cells studied by dielectrophoresis. Biochim Biophys Acta 1146:119-126.

Harris CM, Kell DB. 1983. The radio-frequency dielectric properties of yeast cells measured with a rapid, automated, frequency-domain dielectric spectrometer. Bioelectrochem Bioenerg 11:15-28.

Hölzel R, Lamprecht I. 1992. Dielectric properties of yeast cells as determined by electrorotation. Biochim Biophys Acta 1104:195-200.

Johnk CTA. 1988. Engineering electromagnetic fields and waves, 2nd ed. New York: John Wiley & Sons.

Klösgen B, Reichle C, Kohlsmann S, Kramer KD. 1996. Dielectric spectroscopy as a sensor of membrane headgroup mobility and hydration. Biophys J 71:3251-3260.

Kotnik T, Bobanović F, Miklavčič D. 1997. Sensitivity of transmembrane voltage induced by applied electric fields—a theoretical analysis. Bioelectrochem Bioenerg 43:285-291.

Kotnik T, Miklavčič D, Slivnik T. 1998. Time course of transmembrane voltage induced by time-varying electric fields—a method for theoretical analysis and its application. Bioelectrochem Bioenerg 45:3-16.

Nimtz G, Enders A, Bingelli B. 1985. Hydration dependence of the head group mobility in phospholipid (DMPC) membranes. Ber Bunsenges Phys Chem 89:842-845.

Pauly H, Schwan HP. 1959. Über die Impedanz einer Suspension von kugelförmigen Teilchen mit einer Schale. Z Naturforsch 14B:125-131.

Pottel R, Göpel KD, Henze R, Kaatze U, Uhlendorf V. 1984. The dielectric permittivity spectrum of aqueous colloidal phospholipid solutions between 1 kHz and 60 GHz. Biophys Chem 19:233-244.

Sunderman FW. 1945. Measurement of serum total base. Am J Clin Path 15:219-222.

Ulrich AS, Watts A. 1994. Molecular response of the lipid headgroup to bilayer hydration monitored by ^{2}H-NMR. Biophys J 66:1441-1449.

Vollrath L, Spessert R, Kratzsch T, Keiner M, Hollmann H. 1997. No short-term effects of high-frequency electromagnetic fields on the mammalian pineal gland. Bioelectromagnetics 18:376-387.

Walters TJ, Ryan KL, Belcher JC, Doyle JM, Tehrany MR, Mason PA. 1998. Regional brain heating during microwave exposure (2.06 GHz), warm-water immersion, environmental heating and exercise. Bioelectromagnetics 19:341-353.